



1 **Rubber plant root properties induce contrasting soil aggregate stability**
2 **through cohesive force and reduced land degradation risk in southern China**

3 Waqar Ali¹, Amani Milinga¹, Tao Luo², Mohammad Nauman Khan³, Asad Shah³, Khurram
4 Shehzad⁵, Qiu Yang¹, Huai Yang⁴, Wenxing Long¹, Wenjie Liu^{1*}

5 ¹*Center for Eco-Environment Restoration Engineering of Hainan Province, School of Ecology,*
6 *Hainan University, Haikou, 570228, China.*

7 ²*CSIRO Agriculture and Food, Private Bag 5, Wembley, WA 6913, Australia.*

8 ³*School of Breeding and Multiplication (Sanya Institute of Breeding and Multiplication), Hainan*
9 *University, Haikou, 570228, China*

10 ⁴*Institute of Tropical Bamboo, Rattan & Flower, Sanya Research Base, International Center for*
11 *Bamboo and Rattan, Sanya 572000, China*

12 ⁵*Hubei Key Laboratory of Soil Environment and Pollution Remediation, College of Resources and*
13 *Environment, Huazhong Agricultural University, Wuhan, 430070, China*

14

15

16 *** Corresponding authors:** Wenjie Liu

17 E-mail: liuwj@hainanu.edu.cn

18 Tel: 86-17733181789

19



20 **Abstract**

21 In southern China, Hainan Island faces land degradation risks due to poor soil physical
22 properties, such as a high proportion of microaggregates (< 0.25 mm), low soil organic matter
23 (SOM) content, and frequent uneven rainfall. The cohesive force between soil particles, which is
24 influenced by plant root properties and root-derived SOM, is essential for improving soil aggregate
25 stability and mitigating land degradation. However, the mechanisms by which rubber root
26 properties and root-derived SOM affect soil aggregate stability through cohesive forces in tropical
27 regions remain unclear. This study compared rubber plants of varying ages to assess the effects of
28 root properties and root-derived SOM on soil aggregate stability and cohesive forces. Older rubber
29 plants (> 11 -years-old) showed greater root diameters (RD) (0.81–0.91 mm), higher root length
30 (RL) densities (1.83–2.70 cm/cm³), and increased proportions of fine (0.2–0.5 mm) and medium
31 (0.5–1 mm) roots, leading to higher SOM due to lower lignin and higher cellulose contents. Older
32 plants exhibited higher soil cohesion, with significant correlations among root characteristics,
33 SOM, and cohesive force, whereas the random forest (RF) model identified aggregates (> 0.25
34 mm), root properties, SOM, and cohesive force as the key factors influencing mean weight
35 diameter (MWD) and geometric mean diameter (GMD). Furthermore, partial least squares-path
36 models (PLS-PM) showed that the RL density (RLD) directly influenced SOM (path coefficient
37 0.70) and root-free cohesive force (RFCF) (path coefficient 0.30), which in turn affected the MWD,
38 with additional direct RLD effects on the SOM (path coefficient 0.45) and MWD (path coefficient
39 0.64) in the surface soil. Cohesive force in rubber plants of different ages increased
40 macroaggregates (> 0.25 mm) and decreased microaggregates (< 0.25 mm), with topsoil average
41 MWD following the order: CK (0.98 mm) $<$ 5Y_RF (1.26 mm) $<$ MF (1.31 mm) $<$ 11Y_RF (1.36



42 mm) < 27Y_RF (1.48 mm) < 20Y_RF (1.51 mm). Rubber plant root properties enhance soil
43 aggregate stability and reduce the land degradation risk in tropical regions.

44 **Keywords:** Rubber plant root traits; soil organic matter; cohesive force; aggregate stability; land
45 degradation

46

47 **1. Introduction**

48 Land degradation is a serious global issue that increases as a consequence of growing
49 population and climate change, currently impacting > 75% of land and projected to affect > 90%
50 by 2050 (Perović et al., 2021; Právělie et al., 2021; Thomas et al., 2023). Land degradation in
51 tropical regions, such as Hainan Island, southern China, is primarily caused by poor soil physical
52 properties (high proportion of microaggregates (< 0.25 mm) and low soil organic matter (SOM))
53 along with the uneven and high frequency of rainfall events during the summer season (May–
54 October) and current global climate change, leading to severe land degradation in the form of water
55 erosion (Shao et al., 2024; Zhu et al., 2022). In addition, zonal ferro-alumina lateritic soils
56 (ferralsols) on Hainan Island, classified as having low resilience and sensitivity according to the
57 tropical soil resilience-sensitivity matrix, are particularly prone to soil erosion (Li et al., 2022).
58 Consequently, the current soil erosion area on Hainan Island has increased 4.8-fold compared to
59 that in 2000, according to a third national soil erosion remote-sensing survey (Yu et al., 2016). Soil
60 aggregates are fundamental to soil function, and their stability influences carbon cycling, nutrient
61 storage, soil fertility, infiltration rate, and resistance to soil degradation (Hok et al., 2021; Rabot et
62 al., 2018; Yudina and Kuzyakov, 2023). Therefore, it is imperative to enhance soil aggregate
63 stability by implementing suitable management practices that protect the integrity of the
64 environment and ensure sustainable agricultural productivity.



65 Natural rubber (*Hevea brasiliensis Willd. ex A. Juss*) plantations have recently expanded
66 rapidly across mainland Southeast Asia (Xu et al., 2023; Yang et al., 2024). Rubber plants are
67 recognized for their effectiveness in improving soil aggregate stability through their root properties
68 and in mitigating soil erosion (Kurmi et al., 2020; Sun et al., 2021). Plant roots influence soil
69 aggregate size distribution by positively affecting fine roots length (FRL), which closely interacts
70 with soil particles, and negatively affecting coarse roots length (CRL), which disintegrate into
71 larger particles (Ali et al., 2022; Chen et al., 2021; Kumar et al., 2017). Plant morphological root
72 traits, such as root diameter (RD) and root length (RL) density (RLD), and their chemical
73 composition, including lignin and cellulose content, have been shown to alter carbon deposits in
74 soil pools and their sequestration (Poirier et al., 2018b; Rossi et al., 2020). Nevertheless, various
75 studies have suggested that soil particles and roots have a restricted contact area with plant root-
76 derived SOM, which is a dominant factor in soil particle fluctuation through the soil cohesive force,
77 particularly after the plant roots have died (Ali et al., 2022; Chen et al., 2017). Variations in soil
78 particles and root-derived SOM further adjust soil cohesion.

79 Soil cohesive forces, such as those from SOM and plant root morphological and chemical
80 properties (Wang et al., 2018a; Wang et al., 2020), are effective in stabilizing slope soils to restrain
81 soil and water runoff by enhancing soil-particle interactions, facilitating flocculation between soil
82 particles, and minimizing soil erosion (Smith et al., 2021; Wang et al., 2018a). Among these factors,
83 SOM plays a complex role and is generally beneficial for improving particle flocculation. However,
84 SOM can also allow the dispersion of aggregates owing to an excess charge on SOM coupled with
85 negative charges from soil particles (He et al., 2021; Melo et al., 2021). The addition of plants and
86 their roots allows for additional soil organic carbon (SOC) accumulation in the soil (Rossi et al.,
87 2020). Roots can also bind soil particles via cohesive forces, thus increasing aggregate stability



88 (Forster et al., 2022; Poirier et al., 2018a; Wang et al., 2020). Dominant root traits influence soil
89 particles through cohesive forces, and their subsequent effects on soil aggregate stability remain
90 unknown.

91 To date, few studies on rubber plant roots have focused on soil aggregation in the tropical
92 region of Hainan Island (Sun et al., 2021; Zou et al., 2021), and there is a complete lack of
93 information regarding the mechanisms related to rubber plant root morphological and chemical
94 properties, root-derived SOM, and cohesive forces in aggregate formation. We hypothesized that
95 rubber plantations of different stand ages would promote soil cohesive forces through root
96 properties and SOM among soil particles, thereby improving aggregate stability. The aims of this
97 study were to: 1) investigate the impact of stand-age rubber plant root traits and root-derived SOM
98 on aggregate properties, and 2) explore the interconnections between root morphological and
99 chemical characteristics, SOM, cohesive forces, and soil aggregate stability. The findings of this
100 research will help improve management practices in the tropical regions of Hainan Island and
101 reduce land degradation problems by improving aggregate stability and overall environmental
102 quality.

103

104 **2. Materials and methods**

105 *2.1. Experimental site overview*

106 The study was conducted on Hainan Island in Danzhou (19°4'3''–19°12'42''N, and 109°47'
107 6''–110°1'2''E, 182–255 m above sea level). In the study area, the annual averages for temperature,
108 precipitation, and solar radiation are 23.5°C, 1831 mm, and 4579 MJ·m⁻²·yr⁻¹, respectively.
109 November–April of the following year is the dry season, whereas May–October is the rainy season.
110 Rubber (*Hevea brasiliensis*) and areca (*Areca catechu* L.) are the two primary commercial crops



111 in the experimental region. According to the USA Soil Taxonomy System, the soil is classified as
112 a laterite ferralsol (Schad, 2023). The soil in the rubber plantation was composed of 43.71% sand,
113 8.28% silt, and 48.01% clay. The basic physical and chemical characteristics of the samples are
114 listed in Table. 1.

115 2.2. *Experimental design*

116 Rubber plantations with four different stand ages were selected from the field. The
117 treatments included five-year-old rubber forests (5Y_RF), with 2018 rubber trees (clone PR-107)
118 planted at the recommended density (3×7 m, 480 plants·ha⁻¹) and crown density 30 %; 11-year-
119 old rubber forests (11Y_RF), with 2012 rubber trees (clone PR-107) planted at the recommended
120 density (3×7 m, 431 plants·ha⁻¹) and crown density 90 %; 20-year-old rubber forests (20Y_RF),
121 with 2003 rubber trees (clone PR-107) planted at the recommended density (3×7 m, 346
122 plants·ha⁻¹) and crown density 90 %; 27-year-old rubber forests (27Y_RF), with 1996 rubber trees
123 (clone PR-107) planted at the recommended density (3×7 m, 300 plants·ha⁻¹) and crown density
124 90 %; and mixed forest (MF) and control (no forest plants) (CK). The MF comprised cinnamon
125 (*Cinnamomum Verum*) trees (planted in 2014) along with 20-year-old rubber plants. We established
126 a randomized complete block design with three replicates. We selected 18 plots (30×30 m)
127 separated by a transitional zone. Rubber plants with different stand ages were selected based on
128 similar topographies (slope and gradient) and management practices. Rubber plantation canopy
129 heights were approximately 20 m. The rubber plant rotation duration was approximately 40 yr, and
130 the first latex tapplings in this region occurred when the trees were five- or six-years-old. Chemical
131 fertilizers were applied at the initial rubber plantation development stage according to local
132 conventional farming practices. Additional details regarding the rubber plantations at the
133 experimental site can be found in the study by Sun et al. (2021).



134 *2.3. Root morphological and chemical composition analysis*

135 In January 2024, three replications per depth per forest plot of soil samples with roots were
136 taken at soil depths of 0–20 and 20–40 cm, using cutting rings (200 cm³). Using the methodology
137 outlined by Chen et al. (2021), the following root features were measured: RD, root mass density
138 (RMD), RLD, and root surface area density (RSD). The cutting ring cores were placed in nylon
139 bags and taken to the laboratory, where they were submerged in water for an hour before being
140 manually washed using 0.55-mm sieves to collect the roots. The roots were scanned using an
141 Epson Perfection V800 photo scanner (© 2024 Epson America, Inc), and WinRHIZO Pro Version
142 2009c software was used to assess the RD and RL. By dividing the entire RL and root surface area
143 by the cutting-ring volume (cm³), respectively, the RLD and RSD were calculated. The roots were
144 oven-dried at 50°C, and the RMD was calculated by dividing the dry root mass by the cutting-ring
145 volume. Furthermore, using data from the WinRHIZO analyzer, the root system was classified into
146 four types based on RD: RD < 0.2 mm (very fine roots (VFRL)), RD 0.2–0.5 mm (fine roots
147 (FRL)), RD 0.5–1 mm (medium roots (MRL)), and RD > 1 mm (CRL).

148 Chemical composition (cellulose and lignin) analysis of the roots was performed on three
149 subsamples of the root classes (RD < 0.5, 0.5–1, and > 1 mm). Briefly, 1 mg of 65 °C oven-dried
150 root powder (< 0.5 mm) was mixed with 5 ml acetic acid and heated for 25 min, followed by three
151 deionized water washings and supernatant discarding. Subsequently, 10 ml of sulfuric acid (10%)
152 and 10 ml of potassium dichromic (0.1 mol L⁻¹) solutions were added, vortexed, and heated in a
153 100 °C water bath for 10 min. After cooling, 5 ml KI solution (20%) and 1 ml starch (0.5%) were
154 added, shaken for 10 min, and then titrated with 0.2 mol L⁻¹ sodium thiosulfate to determine
155 cellulose and lignin contents (Zhang et al., 2014).

156



157 *2.4. Soil cohesive force determination*

158 Soil samples of approximately 2000 g were collected from depths of 0–20 and 20–40 cm
159 during root collection. Soil samples were air-dried and divided into two parts. One part was ground
160 to 100 μm for SOM determination using the oxidation method described by Walkley and Black
161 (1934). The second part was dry-sieved to retain aggregates < 5 mm, and visible roots were
162 removed. These soil samples were stored for subsequent analysis of the remolded soil root-free
163 cohesion force (RFCF), which was determined according to the method described by Huang et al.
164 (2022). Briefly, four subsamples of intact root–soil composite cores were collected from each
165 depth in three replicated plots using cutting rings (diameter = 10 cm, height = 6.37 cm)
166 simultaneously during the root collection described in Section 2.3. These intact cores were used to
167 determine soil cohesive forces. Soil cohesive force (c) was measured by assessing soil shear
168 strength (τ) and vertical load (σ) applied to the shear surface, and c was calculated using the
169 relationship between τ , σ , and c as described in Equation 1. In addition, soil (< 5 mm) without
170 visible roots was remolded into cutting rings (diameter = 10 cm, height = 6.37 cm) according to
171 the soil bulk density (Table. 1) at each soil depth in the rubber plots to measure the soil RFCF. In
172 total, 48 core soil samples per treatment were used for soil cohesive force analysis. Both the
173 remolded root-free and root–soil composite core samples were saturated with deionized water.
174 After saturation, four subsamples from each depth and treatment were tested using an LH-DS-4
175 direct shear tester (Nanjing Technology Co., Ltd.), which has a shear strain accuracy of 0.01 mm
176 and a shear stress accuracy of 0.01 N. The shear tester comprised a shear box, a sensor, a vertical
177 compression device, and a displacement measurement system with specifications of 61.8 mm in
178 diameter and a height of 20 mm. For the direct shear tests, four predetermined vertical loads (25,
179 50, 75, and 100 kPa) were applied. The shear rate of displacement was set at 0.8 mm/min, and the



180 soils were sheared until failure, indicated by reaching the peak τ value on the computer. The
181 relationship between the peak τ values and vertical loads (σ) was established according to Mohr–
182 Coulomb’s law, and soil cohesion (c) was calculated as described in Equation 1.

$$183 \quad \tau = c + \sigma \tan\varphi \quad (1)$$

184 where τ is the soil shear strength (kPa), σ is the vertical load applied to the shear surface (kPa), c
185 is the soil cohesive force (kPa), and φ is the soil internal friction angle ($^{\circ}$).

186 *2.5. Soil aggregate analysis*

187 Soil samples from depths of 0–20 and 20–40 cm were collected in each treatment
188 simultaneously with root sample collection. The soil was allowed to air dry and then gently
189 ruptured along its natural cracks before it was passed through an 8 mm mesh sieve to determine
190 the soil aggregate size distribution and stability. We used a wet sieving method to separate
191 aggregates < 8 mm into four size groups: large macroaggregates (LMA) (> 2 mm);
192 macroaggregates (MA) (2–0.25 mm); microaggregates (MIA) (0.25–0.053 mm); and small
193 microaggregates (SMA) (< 0.053 mm). Briefly, three replicates of 100 g of soil were immersed in
194 deionized water for 10 min in a beaker before being transferred to a series of sieves with decreasing
195 mesh sizes (2, 0.25, and 0.053 mm) and gently shaken in water with a 4-cm vertical vibration
196 amplitude for 10 min. Subsequently, the soil that remained after each sieve was washed
197 and transferred to a beaker, and all aggregate sizes (> 2 , 2–0.25, and 0.25–0.053 mm) were oven-
198 dried for 48 hours at 60 $^{\circ}\text{C}$ before being weighed. The mass of aggregates < 0.053 mm was
199 determined by subtracting the total soil mass from the total mass of other aggregate sizes (Elliott,
200 1986). Equations 2 and 3 were used to compute the geometric mean diameter (GMD) and mean
201 weight diameter (MWD, mm), respectively (Kemper and Rosenau, 2018).



202
$$MWD = \sum_{i=1}^n W_i * X_i \quad (2)$$

203 where X_i denotes the mean diameter of aggregate fraction i , and W_i denotes the mass proportion of
204 aggregate fraction i .

205
$$GMD = \exp \left[\sum_{i=1}^n W_i * \ln (X_i) \right] \quad (3)$$

206 where W_i represents the aggregate fraction mass proportion i , and X_i represents the mean diameter
207 of aggregate fraction i .

208 2.6. Statistical analysis

209 Prior to data analysis, Shapiro–Wilk ($P > 0.05$) and Levene's tests ($P > 0.05$) (Razali and
210 Wah, 2011) were used to evaluate the normality and homogeneity of variances using SPSS 25
211 (IBM Corp., Chicago, USA). Origin 2021 software was used to assess each index, and Tukey's
212 pairwise test was used to determine statistical significance at $P < 0.05$, 0.01 , and 0.001 . Pearson's
213 correlations among root characteristics, SOM, soil aggregate parameters, and soil cohesive force
214 were assessed using Origin software (OriginLab Corp.), and key factors were predicted using a
215 random forest (RF) model constructed using the R software RandomForest package (v4.3.1)
216 (Team, 2017). The partial least squares-path models (PLS-PM) were performed in R software
217 (v4.3.1) using the "*plspm*" package to elucidate the pathway through which plant root
218 characteristics, SOM, and soil cohesive forces influence soil aggregate stability. Figures were
219 created using Origin 2021 (OriginLab Corp.).

220

221

222



223 **3 Results**

224 *3.1. Root distribution and chemical composition*

225 Significant differences in root morphological traits were observed among rubber
226 plantations of different stand ages (Fig. 1). The RD varied notably with the age of the rubber plant
227 (Fig. 1a). The largest RD was found in 27Y_RF, followed by the MF at depths of 0–20 cm and
228 20–40 cm, respectively. Specifically, the largest RD for 27Y_RF was 0.84 mm and 0.91 mm at
229 depths of 0–20 cm and 20–40 cm, respectively. By contrast, the smallest RD, found in five-year-
230 old rubber plantations (5Y_RF), ranged from 0.42 to 0.45 mm across both depths, respectively.
231 The differences in RD among rubber plants of varying stand ages depended on soil depth, with the
232 most pronounced differences observed at a depth of 0–20 cm. Moreover, significant variations in
233 RLD were observed between rubber plantations of different stand ages, as shown in Fig. 1b.
234 27Y_RF exhibited the highest RLD, ranging from 1.83 to 2.81 cm/cm³, followed by MF (2.01–
235 2.06 cm/cm³) and 20Y_RF (1.93–2.70 cm/cm³) at both depths. The RLD differences among rubber
236 plants of various stand ages were influenced by soil depth, with the most noticeable differences
237 occurring at a depth of 0–20 cm. In addition, the RSD and RMD were significantly different among
238 rubber plantations of different stand ages (Fig. 1c, and d). Furthermore, RD distribution,
239 represented as a percentage of RL within each RD class, also differed among rubber plantations of
240 various stand ages (Fig. 2). In the 5Y_RF, 11Y_RF, and MF plantations, VFRL (< 0.2 mm)
241 predominated at both soil depths. Conversely, in the 20Y_RF and 27Y_RF plantations, the roots
242 were uniformly distributed across the soil depths, with a relatively high percentage of MRL (0.5–
243 1 mm).

244 The root chemical composition varied among rubber plantations of different stand ages and
245 RD classes (Fig. 3). The cellulose contents in stand-age rubber plants were significantly different
246 (Fig. 3a). The 20Y_RF roots had higher cellulose content than those of the 27Y_RF, followed by



247 the 11Y_RF. Similarly, the cellulose content differed among the RD classes. For example,
248 cellulose in the 5Y_RF was less than that in other stand-age rubber plants for FRL (< 0.5 mm).
249 Moreover, there were significant differences in lignin content among the stand-age rubber plants
250 and between the RD classes (Fig. 3b). For example, the lignin contents in the 20Y_RF were less
251 than that in the 5Y_RF for RL < 0.5 mm. Cellulose and lignin contents are indicators of root
252 contribution to SOM. Thus, the lower lignin and higher cellulose content in the 20Y_RF resulted
253 in the highest SOM content ranging from 21.16 to 23.37 g/kg, followed by that in the 11Y_RF
254 ranging from 20.56 to 22.68 g/kg, and the 27Y_RF ranging from 21.04 to 21.78 g/kg within soil
255 depth (Fig. 3c).

256 *3.2. Soil cohesive force under different stand-age rubber plantations*

257 There was a significant difference in the RFCF among rubber plantations of different stand
258 ages (Fig. 4a). The CK (without plants) RFCF was 17.92 and 20.25 kPa at depths of 0–20 and 20–
259 40 cm, respectively, and the RFCF matrix significantly increased with the introduction of rubber
260 plantations of different stand ages. For example, at 0–10 cm soil depth, compared to the CK, the
261 ability of rubber plants to improve the soil cohesive force followed the order MF > 27Y_RF >
262 20Y_RF > 11Y_RF > 5Y_RF. For the 20Y_RF, the increases in RFCFs relative to the CK were
263 169.73 and 156 % at 0–20 and 20–40 cm, respectively. Generally, older rubber plants (> 11-years-
264 old) yielded a greater RFCF than younger rubber plants.

265 The root–soil composite cohesive force exhibited different patterns among rubber
266 plantations of different stand ages compared to that of the RFCF (Fig. 4b). The root–soil composite
267 cohesive force showed significant differences among rubber plantations of different stand ages and
268 with that in the CK at 0–20 cm depths, whereas the root–soil composite force was significantly
269 greater with plants than with that in the CK at 20–40 cm depth. However, there were no significant



270 differences in the root–soil composite cohesive forces among the different plantations within the
271 20–40 cm soil depth. This is likely because rubber plants of different stand ages (20Y_RF, 27Y_RF,
272 and MF) had greater root–soil interactions, likely due to thicker RD, higher RLD, higher
273 percentage of MRL, and higher SOM at a depth of 0–20 cm. Overall, both cohesive forces were
274 significantly correlated with RLD, VFRL, FRL, and SOM (Fig. 6). These results indicate that
275 rubber plantations of different stand ages have a greater ability to improve soil cohesive forces.

276 *3.3. Soil aggregate properties under different stand-age rubber plantations*

277 Soil aggregate properties exhibited different patterns among the various rubber plant
278 treatments (Fig. 5). Soil aggregates sizes were predominantly 2–0.25 mm, followed by > 2 mm,
279 and 0.25–0.053 mm, and aggregate sizes > 0.0053 mm were less dominant in all rubber plantations
280 of different stand ages compared to that in the CK at the respective soil depths (Fig. 5a–f). In the
281 CK, the percentages of aggregates 2–0.025 mm were 23.76 and 26.84 % at depths of 0–20 and 20–
282 40 cm, respectively. Compared to the CK, rubber plantations of different stand ages showed a
283 significant increase in 2–0.25 mm aggregates at both soil depths. However, the proportion of
284 aggregates > 2 mm, significantly increased in rubber plantations of different stand ages compared
285 to that in the CK at respective soil depths, in the order 20Y_RF > 11Y_RF > 27Y_RF > MF >
286 5Y_RF. Simultaneously, the proportion of aggregates < 0.053 mm was significantly reduced in
287 rubber plantations of different stand ages compared with the CK. As a result of the increase in
288 macroaggregates (> 2 mm) and the decrease in microaggregates (< 0.053 mm) following rubber
289 plantation treatments of varying stand ages, aggregate stability (measured by MWD and GMD)
290 improved to varying extents, in the following order: 20Y_RF > 27Y_RF > 11Y_RF > MF >
291 5Y_RF > CK.

292



293 *3.4 Relationship among root traits, SOM, cohesive force, and soil aggregate stability*

294 The Pearson correlation analysis indicated that the soil RFCF was positively and strongly
295 associated with MWD and GMD with a correlation coefficient of 0.81 and 0.91 (0–20 cm), and
296 0.81 and 0.89 (20–40 cm), whereas the soil RFCF was significantly negatively correlated with
297 small microaggregates (< 0.053 mm) ($r = -0.74$ and -0.79) for both depths (Fig. 6). A similar
298 trend was observed for the root–soil composite cohesive force. Generally, a large cohesive force
299 was consistent with high RLD, high proportions of FRL and MRL, and high SOM, particularly in
300 older rubber plants, and was responsible for its capacity to maintain higher aggregate stability.

301 The RF model further identified the importance of various soil factors in predicting soil
302 aggregate stability (MWD and GMD) at both soil depths (Fig. 7). At both depths, LMA (> 2 mm)
303 and MA (2–0.25 mm) were the most influential factors, contributing significantly to soil stability,
304 followed by SOM and FRL (FRL_0.2–0.5 mm). Root properties and soil cohesive forces also play
305 substantial roles, particularly at deeper soil depths (20–40 cm), where cohesive forces become
306 more prominent. Root traits are essential for enhancing soil aggregate stability, and their impact
307 varies with depth, underscoring the complex interactions between roots and soil structure in
308 ecosystem functions. In addition, the PLS-PM explicated the indirect and direct impact of root
309 properties, SOM, and cohesive forces on soil aggregate stability (Fig. 8). Among the factors
310 measured in the surface soil (0–20 cm), RLD (path coefficient 0.64, $P < 0.05$) directly influenced
311 SOM (path coefficient 0.45, $P < 0.05$) and the MWD. In addition, RLD had a strong direct effect
312 on SOM (path coefficient 0.70, $P < 0.05$). Furthermore, RLD directly altered RFCF (path
313 coefficient 0.30, $P < 0.05$), which further affected the MWD. In contrast, RLD directly influenced
314 the root soil composite cohesive force (RSCCF), however, the RSCCF did not directly influence
315 the MWD. A similar trend was observed in the deep soil (20–40 cm).



316 **4 Discussion**

317 *4.1. Stand-age rubber plant root influence on soil cohesive forces*

318 Rubber plantations of different stand ages exhibited different root morphological traits.
319 Our results demonstrated that the plant roots of rubber plantations aged < 11-years-old were
320 influenced by soil properties at 0–20 and 20–40 cm depths, as indicated by a sharp decline in RD
321 and RLD (Fig. 1), and restricted root growth due to an increase in soil bulk density and a decrease
322 in macropores. Similarly, Sun et al. (2021) observed that at the same research site, older rubber
323 plants (13-years-old) exhibited a preference for growing in macropores compared to younger
324 plants (four-years-old), which was attributed to their superior root properties and lower soil bulk
325 density. In contrast, the 27Y_RF and MF were minimally influenced by soil properties due to the
326 high percentage of FRL and MRL, which likely enlarged medium soil pores and facilitated
327 penetration through capillary soil pores (< 30 μm) (Ali et al., 2022; Chen et al., 2021; He et al.,
328 2022). Older rubber plants possess a higher proportion of FRL and MRL and produce a greater
329 amount of root exudates, which likely function as lubricants to facilitate root growth in compacted
330 soils with a higher bulk density (Chen et al., 2017; Sun et al., 2023). In our study, older rubber
331 plants demonstrated a higher root penetration ability than younger plants, which likely modified
332 the soil cohesive forces.

333 Our results indicate that rubber plant roots of different stand ages were more effective in
334 enhancing soil cohesive forces in tropical regions than in the CK (no rubber plants) (Fig. 4). Many
335 studies have shown that plant roots positively affect soil detachment rates during rainfall events,
336 which can be attributed to an increase in soil cohesive forces (Huang et al., 2022; Shen et al., 2021).
337 Our findings further validate the hypothesis that rubber plantations of different stand ages produce
338 different soil cohesive forces, which are associated with their root characteristics and contributions



339 to SOM. The variation in the enhancement of root–soil composite cohesive forces among rubber
340 plantations of different stand ages was due to their distinct root properties. Younger rubber plants
341 (< 20Y_RF) were more effective at increasing soil cohesion in the topsoil (0–20 cm), whereas
342 older plants improved soil cohesion in both the topsoil and deeper layers compared to that in the
343 CK (Fig. 4) because of their higher root tensile strength, soil shear strength, and greater RD and
344 RLD. However, the RD and RLD of younger plants were significantly reduced in the subsoil,
345 thereby diminishing their impact on soil cohesion. In contrast, older rubber plants enhance soil
346 cohesive forces because of their extensive root contact area with the soil and the high density of
347 their crisscrossing FRL and MRL networks, which effectively bind and wrap soil particles (Huang
348 et al., 2022; Vannoppen et al., 2015, 2017). In the current study, RLD and a substantial proportion
349 of FRL and MRL in older rubber plants enhanced root–soil contact and strengthened the soil at
350 both depths (Figs. 1, and 2).

351 The influence of roots on the cohesive force of root-free soils can be ascribed to their
352 indirect contribution to SOM. Soils from older rubber plantations exhibited high SOM content
353 (Fig. 3c), which enhanced clay particle cohesion by reducing the surface tension of water within
354 the clay–organic matter matrix (Wuddivira et al., 2009). RD and chemical composition (cellulose)
355 altered carbon sequestration in various soil pools, enhancing carbon accumulation in the coarse
356 silt fraction (20–50 μm), while decreasing carbon accumulation in particulate organic matter (Liao
357 et al., 2023; Zhang et al., 2014). Similarly, roots with higher cellulose/lignin ratios facilitate the
358 accessibility of substrates to polymer-hydrolyzing enzymes, thereby accelerating the degradation
359 of plant organic matter (Barto et al., 2010; Halder et al., 2021; Zhang et al., 2014). In addition,
360 root exudates facilitate root penetration into compacted soil layers and increase the distribution
361 frequency of SOM in deeper soil horizons (Oleghe et al., 2017). In general, older rubber plants



362 exhibited a greater RLD, higher percentage of FRL and MRL, and increased SOM than younger
363 rubber plants, which led to a higher RFCF.

364 *4.2. Aggregate stability responses to soil cohesive forces under different stand-age rubber*
365 *plantations*

366 Our study provides comprehensive insights into soil aggregate stability across rubber
367 plantations at different stages of stand maturity. Soil cohesive forces driven by plant root traits are
368 key factors in enhancing soil aggregate stability. The soil cohesive force increased aggregate
369 stability (MWD and GMD) at the same soil depth (Fig. 5). The results also indicated that cohesive
370 forces not only governed macroaggregate stability but also played a role in microaggregate
371 formation. The MWD increased across rubber plantations of different stand ages because of the
372 significant enhancement in soil cohesive forces. Rubber plants older than 11 years exhibited the
373 highest aggregate stability at the same soil depth, which was consistent with the trend observed in
374 their RFCF (Fig. 4). High soil cohesion has also been documented to limit soil dispersion rates and
375 mitigate gully erosion (Wuddivira et al., 2013). Although the soil RFCCF was highest in older
376 rubber plantations, the highest SOM content likely played a positive role in stabilizing soil particles
377 (Kamau et al., 2020). SOM had a positive effect on soil particles as its dispersive properties became
378 evident only once the soil aggregates were broken down. High SOM content also weakens the
379 electrostatic repulsive forces by influencing the overlap of oppositely charged electric double
380 layers (Ali et al., 2023; Yu et al., 2020). In addition, the higher MWD observed in rubber
381 plantations older than 11 years, compared to those in the 5Y_RF and CK, indicated that the MWD
382 of older rubber plants was not adversely affected by the excessive release of SOC from the
383 mechanical breakdown of macroaggregates.

384 These findings highlight the importance of understanding the specific mechanisms by
385 which soil cohesive forces contribute to aggregate stability. In this study, the soil aggregate portion



386 (< 0.25 mm) was comparatively higher in the rubber plantations than in the control in this study.
387 Rubber plant roots and SOM positively enhanced cohesion between soil particles (Fig. 5a–f). The
388 soil cohesive force regulates soil aggregate stability using the following approaches: First, smaller
389 aggregates, due to their higher surface area to volume ratio with water, can create surface tension
390 between particles, indirectly creating a cohesive force, helping to hold them together (Wang et al.,
391 2023). Second, soil particles, particularly clay and organic matter, often carry electrical charges
392 that can lead to electrostatic attraction, further stabilizing the soil particles (Kaiser and Asefaw
393 Berhe, 2014; Wuddivira et al., 2009). Similarly, SOM has a positive effect on clays because the
394 dispersive effect of SOM is not expressed until the aggregates are broken (Melo et al., 2021). High
395 SOM also weakens the electrostatic repulsive force in ultisols through its additional impact on the
396 overlap of oppositely charged electric double layers (Ali et al., 2023; He et al., 2021; Yu et al.,
397 2020). Third, the water in the small pores between the soil particles creates a capillary force that
398 contributes to the soil cohesive force, which agglomerates the small particles (Deviren Saygin et
399 al., 2021). In general, stand-age rubber plantations positively improved soil aggregate stability
400 compared to the control through soil cohesion. In young rubber plantations, legumes such as kudzu
401 should be planted. Furthermore, the development of a forest rubber understory economy can
402 significantly enhance soil health by increasing biodiversity, with diverse plant roots improving soil
403 structure, promoting microbial activity, preventing erosion, and contributing to organic matter
404 through leaf litter and root biomass, thereby improving soil fertility. Future research should focus
405 on evaluating the mechanisms by which various understory plants in rubber plantations reduce soil
406 erosion.
407
408



409 5. Conclusion

410 In this study, we explored the potential mechanisms of different stand-age rubber plant root
411 morphological properties, root-derived SOM, and root chemical compositions on soil aggregate
412 stability improvement through soil cohesive forces. Our findings indicate that natural rubber
413 plantations of different stand ages exhibit distinct root distribution patterns, with 27-year-old
414 rubber forests (27Y_RF) and MF showing greater RLD and higher percentages of FRL and MRL
415 RD classes than those of younger plantations. The higher percentages of FRL and MRL in older
416 rubber plants (> 11-years-old), along with their high SOM content, contributed to a stronger soil
417 cohesive force than that observed in younger rubber plants and the control plots. The higher SOM
418 content in older rubber plants was driven by the higher cellulose content and lower lignin
419 percentages in their FRL and MRL. Consequently, rubber plants older than 11 years increased the
420 soil cohesive force (with and without roots) compared to younger rubber plants and the control,
421 thereby enhancing aggregate stability and reducing soil particle dispersion. These findings have
422 significant practical implications and may assist in the development of management policies aimed
423 at restoring the soil quality of degraded land in the tropical regions of Hainan Island. They
424 emphasize the importance of selecting rubber plants with optimal root characteristics to enhance
425 aggregate stability through soil cohesive force, thereby sustaining long-term agricultural
426 productivity and maintaining environmental quality.

427 Credit authorship contribution statement

428 **Waqar Ali:** Writing - original draft, visualization, Investigation, Data curation, formal analysis.

429 **Amani Milinga:** Investigation, Data curation. **Tao Luo:** visualization, formal analysis,

430 **Mohammad Nauman Khan:** Writing – review & editing. **Asad Shah:** Writing – review &

431 editing. **Khurram Shehzad:** Investigation, formal analysis. **Qiu Yang:** Investigation, Funding



432 acquisition, review & editing. **Huai Yang:** Writing – review & editing, **Wenxing Long:**
433 Investigation, Data curation. **Wenjie Liu:** Validation, Supervision, Resources, Conceptualization,
434 Funding acquisition.

435 **Declaration of Competing Interest**

436 The authors declare that they have no known competing financial interests or personal
437 relationships that could have appeared to influence the work reported in this paper.

438 **Data availability**

439 Data will be made available on request.

440 **Acknowledgment**

441 This work was financially supported by the National Key Research and Development Program of
442 China (2021YFD2200403-04), and the National Natural Science Foundation of China (No.
443 42367034 and 32160291).

444 **References**

445 Ali, W., Yang, M., Long, Q., Hussain, S., Chen, J., Clay, D., and He, Y.: Different fall/winter
446 cover crop root patterns induce contrasting red soil (Ultisols) mechanical resistance through
447 aggregate properties, *Plant and Soil*, 477, 461–474, <https://doi.org/10.1007/s11104-022-05430-4>,
448 2022.

449 Ali, W., Hussain, S., Chen, J., Hu, F., Liu, J., He, Y., and Yang, M.: Cover crop root-derived
450 organic carbon influences aggregate stability through soil internal forces in a clayey red soil,
451 *Geoderma*, 429, 116271, <https://doi.org/10.1016/j.geoderma.2022.116271>, 2023.

452 Barto, E. K., Alt, F., Oelmann, Y., Wilcke, W., and Rillig, M. C.: Contributions of biotic and
453 abiotic factors to soil aggregation across a land use gradient, *Soil Biology and Biochemistry*, 42,
454 2316–2324, <https://doi.org/10.1016/j.soilbio.2010.09.008>, 2010.



- 455 Chen, C., Liu, W., Jiang, X., and Wu, J.: Effects of rubber-based agroforestry systems on soil
456 aggregation and associated soil organic carbon: Implications for land use, *Geoderma*, 299, 13–24,
457 <https://doi.org/10.1016/j.geoderma.2017.03.021>, 2017.
- 458 Chen, J., Wu, Z., Zhao, T., Yang, H., Long, Q., and He, Y.: Rotation crop root performance and
459 its effect on soil hydraulic properties in a clayey Utisol, *Soil and Tillage Research*, 213, 105136,
460 <https://doi.org/10.1016/j.still.2021.105136>, 2021.
- 461 Deviren Saygin, S., Arı, F., Temiz, Ç., Arslan, Ş., Ünal, M. A., and Erpul, G.: Analysis of soil
462 cohesion by fluidized bed methodology using integrable differential pressure sensors for a wide
463 range of soil textures, *Computers and Electronics in Agriculture*, 191,
464 <https://doi.org/10.1016/j.compag.2021.106525>, 2021.
- 465 Elliott, E. T.: Aggregate Structure and Carbon, Nitrogen, and Phosphorus in Native and Cultivated
466 Soils, *Soil Science Society of America Journal*, 50, 627–633,
467 <https://doi.org/10.2136/sssaj1986.03615995005000030017x>, 1986.
- 468 Forster, M., Ugarte, C., Lamandé, M., and Faucon, M.-P.: Root traits of crop species contributing
469 to soil shear strength, *Geoderma*, 409, 115642, <https://doi.org/10.1016/j.geoderma.2021.115642>,
470 2022.
- 471 Halder, M., Liu, S., Zhang, Z. B., Guo, Z. C., and Peng, X. H.: Effects of residue stoichiometric,
472 biochemical and C functional features on soil aggregation during decomposition of eleven organic
473 residues, *CATENA*, 202, 105288, <https://doi.org/10.1016/j.catena.2021.105288>, 2021.
- 474 He, Y., Yang, M., Huang, R., Wang, Y., and Ali, W.: Soil organic matter and clay zeta potential
475 influence aggregation of a clayey red soil (Ultisol) under long-term fertilization, *Scientific Reports*,
476 11, 20498, <https://doi.org/10.1038/s41598-021-99769-w>, 2021.
- 477 He, Y., Wu, Z., Zhao, T., Yang, H., Ali, W., and Chen, J.: Different plant species exhibit



478 contrasting root traits and penetration to variation in soil bulk density of clayey red soil, *Agronomy*
479 *Journal*, 114, 867–877, <https://doi.org/10.1002/agj2.20972>, 2022.

480 Hok, L., de Moraes Sá, J. C., Boulakia, S., Reyes, M., de Oliveira Ferreira, A., Elie Tivet, F., Saab,
481 S., Aucaise, R., Massao Inagaki, T., Schimiguel, R., Aparecida Ferreira, L., Briedis, C., Santos
482 Canalli, L. B., Kong, R., and Leng, V.: Dynamics of soil aggregate-associated organic carbon
483 based on diversity and high biomass-C input under conservation agriculture in a savanna
484 ecosystem in Cambodia, *CATENA*, 198, 105065, <https://doi.org/10.1016/j.catena.2020.105065>,
485 2021.

486 Huang, M., Sun, S., Feng, K., Lin, M., Shuai, F., Zhang, Y., Lin, J., Ge, H., Jiang, F., and Huang,
487 Y.: Effects of *Neyraudia reynaudiana* roots on the soil shear strength of collapsing wall in
488 Benggang, southeast China, *Catena*, 210, 105883, <https://doi.org/10.1016/j.catena.2021.105883>,
489 2022.

490 Kaiser, M. and Asefaw Berhe, A.: How does sonication affect the mineral and organic constituents
491 of soil aggregates? - A review, *Journal of Plant Nutrition and Soil Science*, 177, 479–495,
492 <https://doi.org/10.1002/jpln.201300339>, 2014.

493 Kamau, S., Barrios, E., Karanja, N. K., Ayuke, F. O., and Lehmann, J.: Dominant tree species and
494 earthworms affect soil aggregation and carbon content along a soil degradation gradient in an
495 agricultural landscape, *Geoderma*, 359, 113983, <https://doi.org/10.1016/j.geoderma.2019.113983>,
496 2020.

497 Kemper, W. D. and Rosenau, R. C.: Aggregate Stability and Size Distribution, in: *Agronomy*
498 *Monograph*, vol. 9, 425–442, <https://doi.org/10.2136/sssabookser5.1.2ed.c17>, 2018.

499 Kumar, A., Dorodnikov, M., Splettstößer, T., Kuzyakov, Y., and Pausch, J.: Effects of maize roots
500 on aggregate stability and enzyme activities in soil, *Geoderma*, 306, 50–57,



- 501 <https://doi.org/10.1016/j.geoderma.2017.07.007>, 2017.
- 502 Kurmi, B., Nath, A. J., Lal, R., and Das, A. K.: Water stable aggregates and the associated active
503 and recalcitrant carbon in soil under rubber plantation, *Science of the Total Environment*, 703,
504 135498, <https://doi.org/10.1016/j.scitotenv.2019.135498>, 2020.
- 505 Li, T., Hong, X., Liu, S., Wu, X., Fu, S., Liang, Y., Li, J., Li, R., Zhang, C., Song, X., Zhao, H.,
506 Wang, D., Zhao, F., Ruan, Y., and Ju, X.: Cropland degradation and nutrient overload on Hainan
507 Island: A review and synthesis, *Environmental Pollution*, 313, 120100,
508 <https://doi.org/10.1016/j.envpol.2022.120100>, 2022.
- 509 Liao, J., Yang, X., Dou, Y., Wang, B., Xue, Z., Sun, H., Yang, Y., and An, S.: Divergent
510 contribution of particulate and mineral-associated organic matter to soil carbon in grassland,
511 *Journal of Environmental Management*, 344, 118536,
512 <https://doi.org/10.1016/j.jenvman.2023.118536>, 2023.
- 513 Melo, T. R. de, Figueiredo, A., and Filho, J. T.: Clay behavior following macroaggregate
514 breakdown in Ferralsols, *Soil and Tillage Research*, 207, 104862,
515 <https://doi.org/10.1016/j.still.2020.104862>, 2021.
- 516 Nornadiah Mohd Razali Yap Bee Wah: Power comparisons of Shapiro-Wilk, Kolmogorov-
517 Smirnov, Lilliefors and Anderson-Darling tests, *Journal of Statistical Modeling and Analytics*, 21–
518 33, 2011.
- 519 Oleghe, E., Naveed, M., Baggs, E. M., and Hallett, P. D.: Plant exudates improve the mechanical
520 conditions for root penetration through compacted soils, *Plant and Soil*, 421, 19–30,
521 <https://doi.org/10.1007/s11104-017-3424-5>, 2017.
- 522 Perović, V., Kadović, R., Đurđević, V., Pavlović, D., Pavlović, M., Čakmak, D., Mitrović, M., and
523 Pavlović, P.: Major drivers of land degradation risk in Western Serbia: Current trends and future



524 scenarios, *Ecological Indicators*, 123, 107377, <https://doi.org/10.1016/j.ecolind.2021.107377>,
525 2021.

526 Poirier, V., Roumet, C., Angers, D. A., and Munson, A. D.: Species and root traits impact
527 macroaggregation in the rhizospheric soil of a Mediterranean common garden experiment, *Plant*
528 and *Soil*, 424, 289–302, <https://doi.org/10.1007/s11104-017-3407-6>, 2018a.

529 Poirier, V., Roumet, C., and Munson, A. D.: The root of the matter: Linking root traits and soil
530 organic matter stabilization processes, *Soil Biology and Biochemistry*, 120, 246–259,
531 <https://doi.org/10.1016/j.soilbio.2018.02.016>, 2018b.

532 Prăvălie, R., Nita, I.-A., Patriche, C., Niculiță, M., Birsan, M.-V., Roșca, B., and Bandoc, G.:
533 Global changes in soil organic carbon and implications for land degradation neutrality and climate
534 stability, *Environmental Research*, 201, 111580, <https://doi.org/10.1016/j.envres.2021.111580>,
535 2021.

536 Rabot, E., Wiesmeier, M., Schlüter, S., and Vogel, H.-J.: Soil structure as an indicator of soil
537 functions: A review, *Geoderma*, 314, 122–137, <https://doi.org/10.1016/j.geoderma.2017.11.009>,
538 2018.

539 Rossi, L. M. W., Mao, Z., Merino-Martín, L., Roumet, C., Fort, F., Taugourdeau, O., Boukcim,
540 H., Fourtier, S., Del Rey-Granado, M., Chevallier, T., Cardinael, R., Fromin, N., and Stokes, A.:
541 Pathways to persistence: plant root traits alter carbon accumulation in different soil carbon pools,
542 *Plant and Soil*, 452, 457–478, <https://doi.org/10.1007/s11104-020-04469-5>, 2020.

543 Schad, P.: World Reference Base for Soil Resources—Its fourth edition and its history, *Journal of*
544 *Plant Nutrition and Soil Science*, 186, 151–163, <https://doi.org/10.1002/jpln.202200417>, 2023.

545 Shao, W., Zhang, Z., Guan, Q., Yan, Y., and Zhang, J.: Comprehensive assessment of land
546 degradation in the arid and semiarid area based on the optimal land degradation index model,



- 547 CATENA, 234, 107563, <https://doi.org/10.1016/j.catena.2023.107563>, 2024.
- 548 Shen, N., Wang, Z., Guo, Q., Zhang, Q., Wu, B., Liu, J., Ma, C., Delang, C. O., and Zhang, F.:
549 Soil detachment capacity by rill flow for five typical loess soils on the Loess Plateau of China,
550 Soil and Tillage Research, 213, 105159, <https://doi.org/10.1016/j.still.2021.105159>, 2021.
- 551 Smith, D. J., Wynn-Thompson, T. M., Williams, M. A., and Seiler, J. R.: Do roots bind soil?
552 Comparing the physical and biological role of plant roots in fluvial streambank erosion: A mini-
553 JET study, Geomorphology, 375, 107523, <https://doi.org/10.1016/j.geomorph.2020.107523>, 2021.
- 554 Sun, R., Wu, Z., Lan, G., Yang, C., and Fraedrich, K.: Effects of rubber plantations on soil
555 physicochemical properties on Hainan Island, China, Journal of Environmental Quality, 50, 1351–
556 1363, <https://doi.org/10.1002/jeq2.20282>, 2021.
- 557 Sun, R., Lan, G., Yang, C., Wu, Z., Chen, B., and Fraedrich, K.: Soil quality variation and its
558 driving factors within tropical forests on Hainan Island, China, Land Degradation and
559 Development, 34, 3418–3432, <https://doi.org/10.1002/ldr.4693>, 2023.
- 560 Team, R. C.: a Language and Environment for Statistical Computing, 2017.
- 561 Thomas, A., Bentley, L., Feeney, C., Lofts, S., Robb, C., Rowe, E. C., Thomson, A., Warren-
562 Thomas, E., and Emmett, B.: Land degradation neutrality: Testing the indicator in a temperate
563 agricultural landscape, Journal of Environmental Management, 346, 118884,
564 <https://doi.org/10.1016/j.jenvman.2023.118884>, 2023.
- 565 Vannoppen, W., Vanmaercke, M., De Baets, S., and Poesen, J.: A review of the mechanical effects
566 of plant roots on concentrated flow erosion rates, Earth-Science Reviews, 150, 666–678,
567 <https://doi.org/10.1016/j.earscirev.2015.08.011>, 2015.
- 568 Vannoppen, W., De Baets, S., Keeble, J., Dong, Y., and Poesen, J.: How do root and soil
569 characteristics affect the erosion-reducing potential of plant species?, Ecological Engineering, 109,



- 570 186–195, <https://doi.org/10.1016/j.ecoleng.2017.08.001>, 2017.
- 571 Walkley, A. and Black, I. A.: An examination of the degtjareff method for determining soil organic
572 matter, and a proposed modification of the chromic acid titration method, *Soil Science*, 37, 29–38,
573 <https://doi.org/10.1097/00010694-193401000-00003>, 1934.
- 574 Wang, B., Zhang, G.-H., Yang, Y.-F., Li, P.-P., and Liu, J.-X.: Response of soil detachment
575 capacity to plant root and soil properties in typical grasslands on the Loess Plateau, *Agriculture,
576 Ecosystems & Environment*, 266, 68–75, <https://doi.org/10.1016/j.agee.2018.07.016>, 2018a.
- 577 Wang, B., Zhang, G.-H., Yang, Y.-F., Li, P.-P., and Liu, J.-X.: The effects of varied soil properties
578 induced by natural grassland succession on the process of soil detachment, *CATENA*, 166, 192–
579 199, <https://doi.org/10.1016/j.catena.2018.04.007>, 2018b.
- 580 Wang, G., Huang, Y., Li, R., Chang, J., and Fu, J.: Influence of Vetiver Root System on
581 Mechanical Performance of Expansive Soil: Experimental Studies, *Advances in Civil Engineering*,
582 2020, 1–11, <https://doi.org/10.1155/2020/2027172>, 2020a.
- 583 Wang, G. Y., Huang, Y. G., Li, R. F., Chang, J. M., and Fu, J. L.: Influence of vetiver root on
584 strength of expansive soil-experimental study, *PLoS ONE*, 15, 1–20,
585 <https://doi.org/10.1371/journal.pone.0244818>, 2020b.
- 586 Wang, J., Wei, H., Huang, J., He, T., and Deng, Y.: Soil aggregate stability and its response to
587 overland runoff–sediment transport in karst peak–cluster depressions, *Journal of Hydrology*, 620,
588 129437, <https://doi.org/10.1016/j.jhydrol.2023.129437>, 2023.
- 589 Wuddivira, M. N., Stone, R. J., and Ekwue, E. I.: Clay, Organic Matter, and Wetting Effects on
590 Splash Detachment and Aggregate Breakdown under Intense Rainfall, *Soil Science Society of
591 America Journal*, 73, 226–232, <https://doi.org/10.2136/sssaj2008.0053>, 2009.
- 592 Wuddivira, M. N., Stone, R. J., and Ekwue, E. I.: Influence of cohesive and disruptive forces on



593 strength and erodibility of tropical soils, *Soil and Tillage Research*, 133, 40–48,
594 <https://doi.org/10.1016/j.still.2013.05.012>, 2013.

595 Xu, W., Liu, W., Tang, S., Yang, Q., Meng, L., Wu, Y., Wang, J., Wu, L., Wu, M., Xue, X., Wang,
596 W., and Luo, W.: Long-term partial substitution of chemical nitrogen fertilizer with organic
597 fertilizers increased SOC stability by mediating soil C mineralization and enzyme activities in a
598 rubber plantation of Hainan Island, China, *Applied Soil Ecology*, 182, 104691,
599 <https://doi.org/10.1016/j.apsoil.2022.104691>, 2023.

600 Yang, Q., Li, J., Xu, W., Wang, J., Jiang, Y., Ali, W., and Liu, W.: Substitution of Inorganic
601 Fertilizer with Organic Fertilizer Influences Soil Carbon and Nitrogen Content and Enzyme
602 Activity under Rubber Plantation, *Forests*, 15, 756, <https://doi.org/10.3390/f15050756>, 2024.

603 Yu, Z., Zheng, Y., Zhang, J., Zhang, C., Ma, D., Chen, L., and Cai, T.: Importance of soil
604 interparticle forces and organic matter for aggregate stability in a temperate soil and a subtropical
605 soil, *Geoderma*, 362, 114088, <https://doi.org/10.1016/j.geoderma.2019.114088>, 2020.

606 Yudina, A. and Kuzyakov, Y.: Dual nature of soil structure: The unity of aggregates and pores,
607 *Geoderma*, 434, 116478, <https://doi.org/10.1016/j.geoderma.2023.116478>, 2023.

608 Zhang, C.-B., Chen, L.-H., and Jiang, J.: Why fine tree roots are stronger than thicker roots: The
609 role of cellulose and lignin in relation to slope stability, *Geomorphology*, 206, 196–202,
610 <https://doi.org/10.1016/j.geomorph.2013.09.024>, 2014.

611 Zhu, X., Liu, W., Yuan, X., Chen, C., Zhu, K., Zhang, W., and Yang, B.: Aggregate stability and
612 size distribution regulate rainsplash erosion: Evidence from a humid tropical soil under different
613 land-use regimes, *Geoderma*, 420, 115880, <https://doi.org/10.1016/j.geoderma.2022.115880>,
614 2022.

615 Zou, X., Zhu, X., Zhu, P., Singh, A. K., Zakari, S., Yang, B., Chen, C., and Liu, W.: Soil quality



616 assessment of different *Hevea brasiliensis* plantations in tropical China, *Journal of Environmental*
 617 *Management*, 285, 112147, <https://doi.org/10.1016/j.jenvman.2021.112147>, 2021.

618

619 **Table captions**

620 **Table 1.** Basic physical and chemical characteristics of the experimental site.

Treatments	Soil depth (cm)	pH	BD (g/cm ³)	TOP (%)	SMC (%)	SOM (g/kg)	AN (mg/kg)	AP (mg/kg)	AK (mg/kg)
CK	0 -20	4.17	1.52	26.37	17.46	12.34	11.92	1.69	24.42
	20 - 40	4.21	1.56	23.26	15.25	11.36	11.45	1.56	18.15
5Y_RF	0 -20	4.37	1.39	28.39	19.25	20.98	11.63	2.79	34.62
	20 - 40	4.13	1.52	23.01	17.63	16.30	10.67	1.73	17.97
11Y_RF	0 -20	3.89	1.43	24.81	21.67	22.68	11.84	2.31	25.23
	20 - 40	4.02	1.51	23.1	20.77	20.56	10.42	1.7	16.44
20Y_RF	0 -20	4.08	1.36	24.98	21.41	23.37	10.67	2.33	29.02
	20 - 40	4.22	1.43	20.31	20.2	21.16	10.39	1.99	23.12
27Y_RF	0 -20	4.08	1.32	25.05	23.68	21.78	11.77	2.39	25.83
	20 - 40	4.26	1.41	25.24	19.9	21.04	10.17	1.84	18.92
MF	0 -20	4.42	1.31	29.52	22.76	21.20	13.47	1.81	36.15
	20 - 40	4.35	1.39	26.58	20.11	20.29	12.84	1.33	19.94

621 Note: BD: Bulk density; TOP: Total porosity; SMC: Soil moisture content; SOM: Soil organic matter; AN: Available nitrogen; AP:
 622 Available phosphorus; AK: Available potassium.

623 **Figure captions**

624 **Figure 1.** Different stand-age rubber plantation root morphological properties with soil depths.

625 **Figure 2.** Root diameter distribution of rubber plants at different stand ages represented by the



626 root length percentage across four class diameters.

627 **Figure. 3.** Different stand-age rubber plantation root chemical compositions and soil organic
628 matter (SOM) distributions.

629 **Figure. 4.** Soil cohesive force distribution under different stand-age rubber plantations. (a) Root
630 free cohesive force, (b) Root–soil composite cohesive force.

631 **Figure. 5.** Different stand-age rubber plantation aggregate size distributions and soil aggregate
632 stabilities (MWD and GWD) with soil depths.

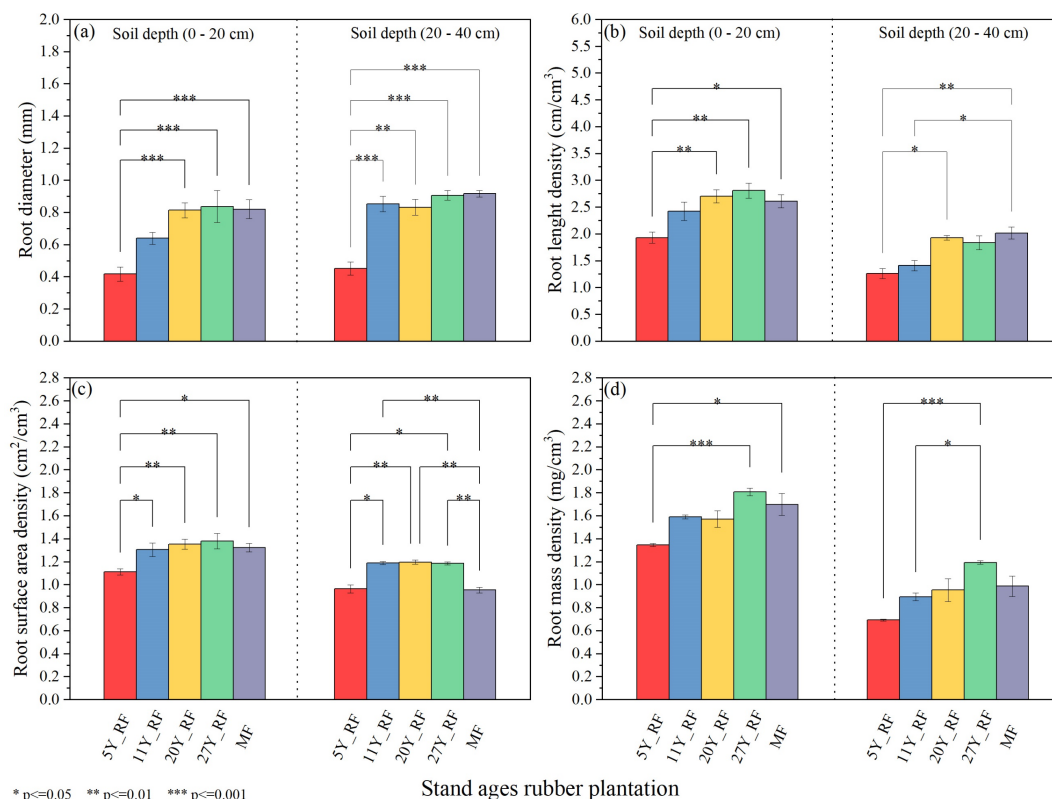
633 **Figure. 6.** Pearson correlations ($P < 0.05$) for all root traits, aggregate stabilities, soil organic
634 matter, and soil cohesive forces. RD: root diameter; RLD: root length density; RSD: root surface
635 area density; RMD: root mass density; VFRL: very fine root length; FRL: fine root length; MRL:
636 medium root length; CRL: coarse root length; SOM: soil organic matter; RFCF: root-free cohesive
637 force; RSCCF: root–soil composite cohesive force; LMA: large macroaggregates (> 2 mm); MA:
638 macroaggregates (2–0.25 mm); MIA: microaggregates (0.25–0.053 mm); SMA: small
639 microaggregates (< 0.053 mm); GMD: geometric mean diameter; MWD: mean weight diameter.
640 The dark brown color indicates a positive correlation, and the pine green color indicates a negative
641 correlation.

642 **Figure. 7.** Random forest model ($P < 0.05$) to identify the key predictors of mean weight diameter
643 (MWD) and geometric mean diameter (GMD). RD: root diameter; RLD: root length density; RSD:
644 root surface area density; RMD: root mass density; VFRL: very fine root length; FRL: fine root
645 length; MRL: medium root length; CRL: coarse root length; SOM: soil organic matter; RFCF root-
646 free cohesive force; RSCCF: root–soil composite cohesive force; LMA: large macroaggregates ($>$
647 2 mm); MA: macroaggregates (2–0.25 mm); MIA: microaggregates (0.25– 0.053 mm); SMA:
648 small microaggregates (< 0.053 mm).



649 **Figure. 8.** Partial least squares-path models (PLS-PM) ($P < 0.05$) indicating the indirect and direct
 650 impact of root properties, soil organic matter, and cohesive forces on soil aggregate stability at 0–
 651 20 cm (a, and b) and 20–40 cm (c, and d). The numbers near the arrows are standardized path
 652 coefficients. The blue line indicates the positive direction and the red line indicates the negative
 653 direction. RD: root diameter; RLD: root length density; SOM: soil organic matter; RFCF: root-
 654 free cohesive force; RSCCF: root–soil composite cohesive force; MWD: mean weight diameter.

655 **Figure. 1.**



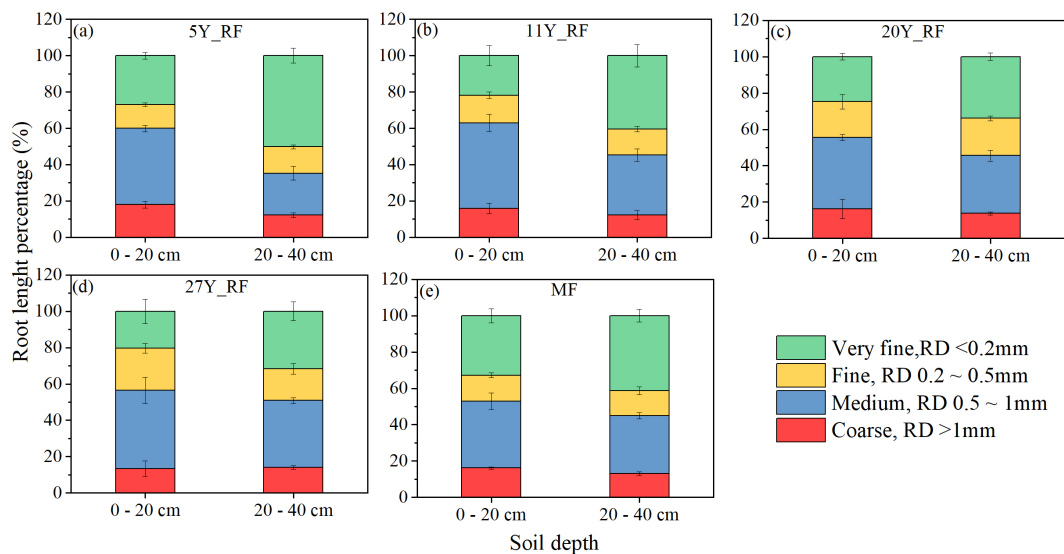
656

* $p < 0.05$ ** $p < 0.01$ *** $p < 0.001$

Stand ages rubber plantation

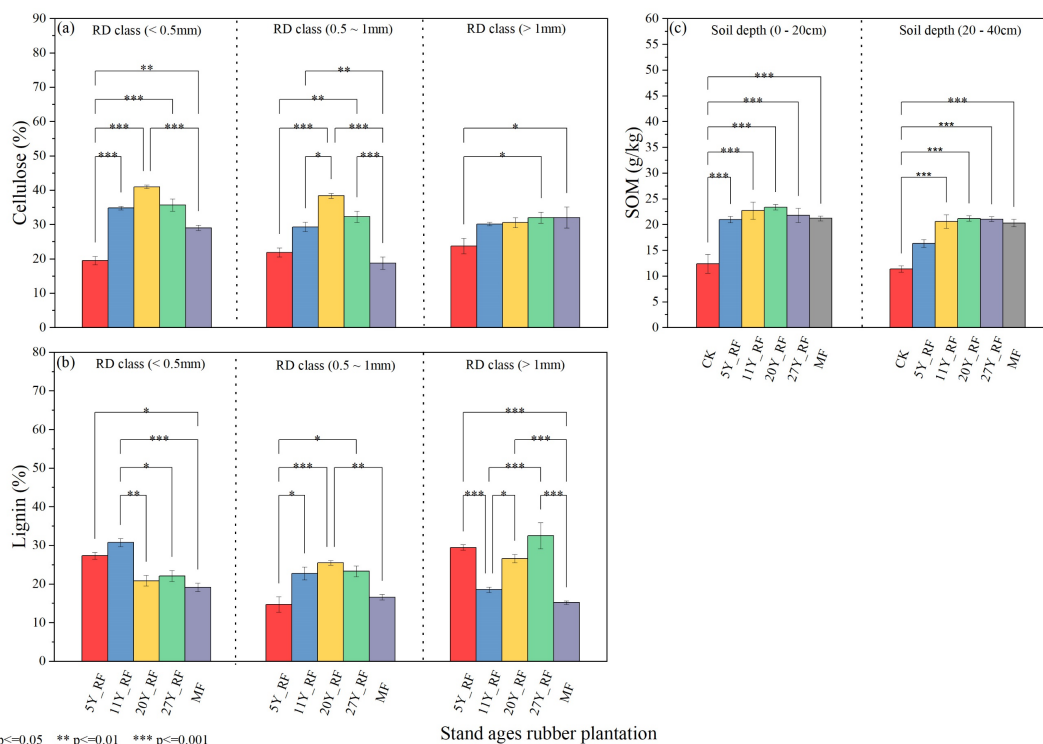
657

658 **Figure. 2.**



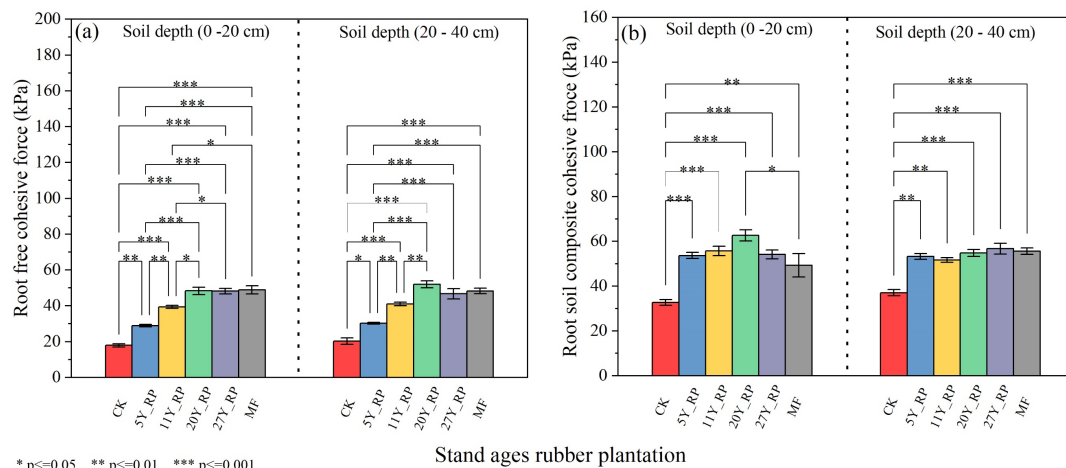
659

660 **Figure 3.**



661

662 **Figure 4.**



663

664

665

666

667

668

669

670

671

672

673

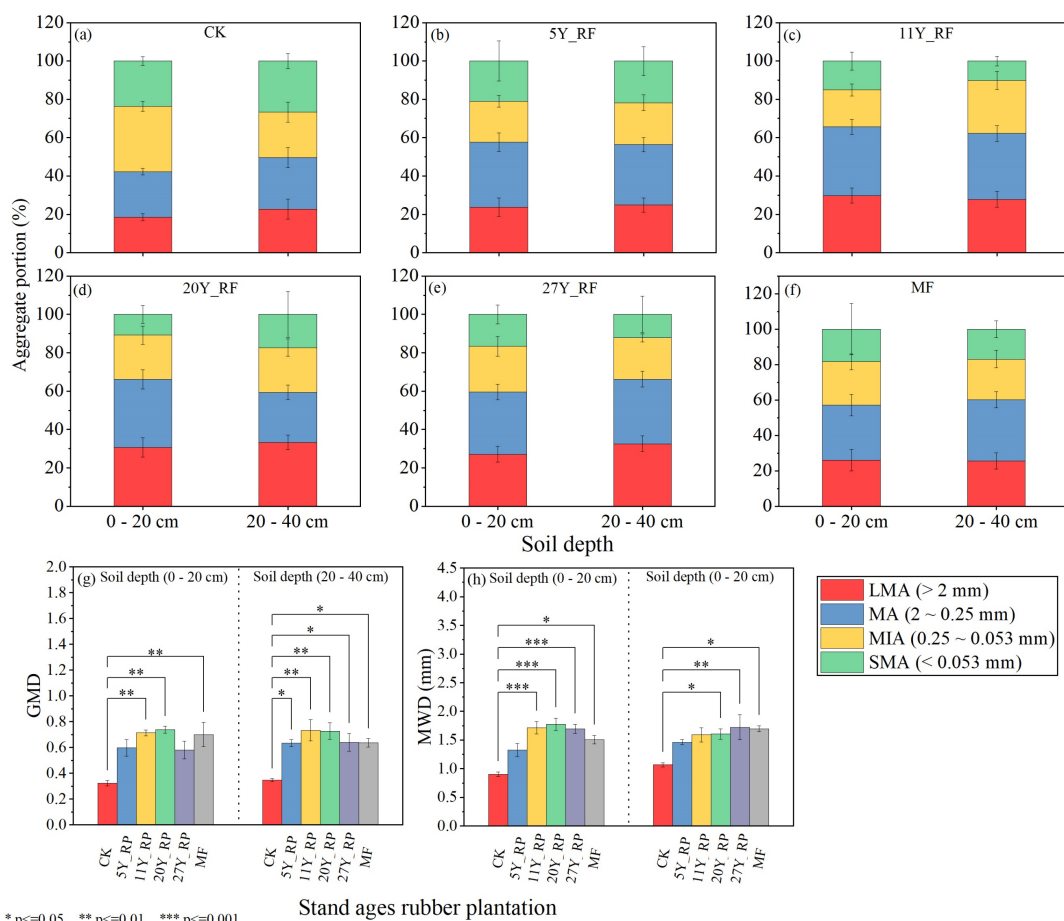
674

675

676

677

678 **Figure 5.**



679 * p<=0.05 ** p<=0.01 *** p<=0.001

680

681

682

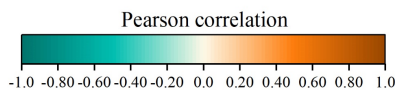
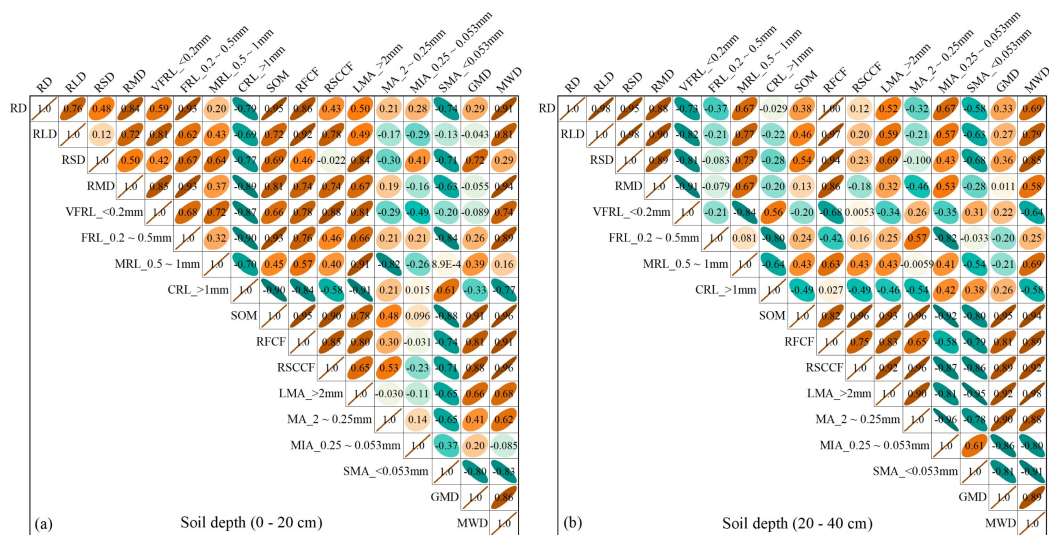
683

684

685

686

687 **Figure. 6.**



688

689

690

691

692

693

694

695

696

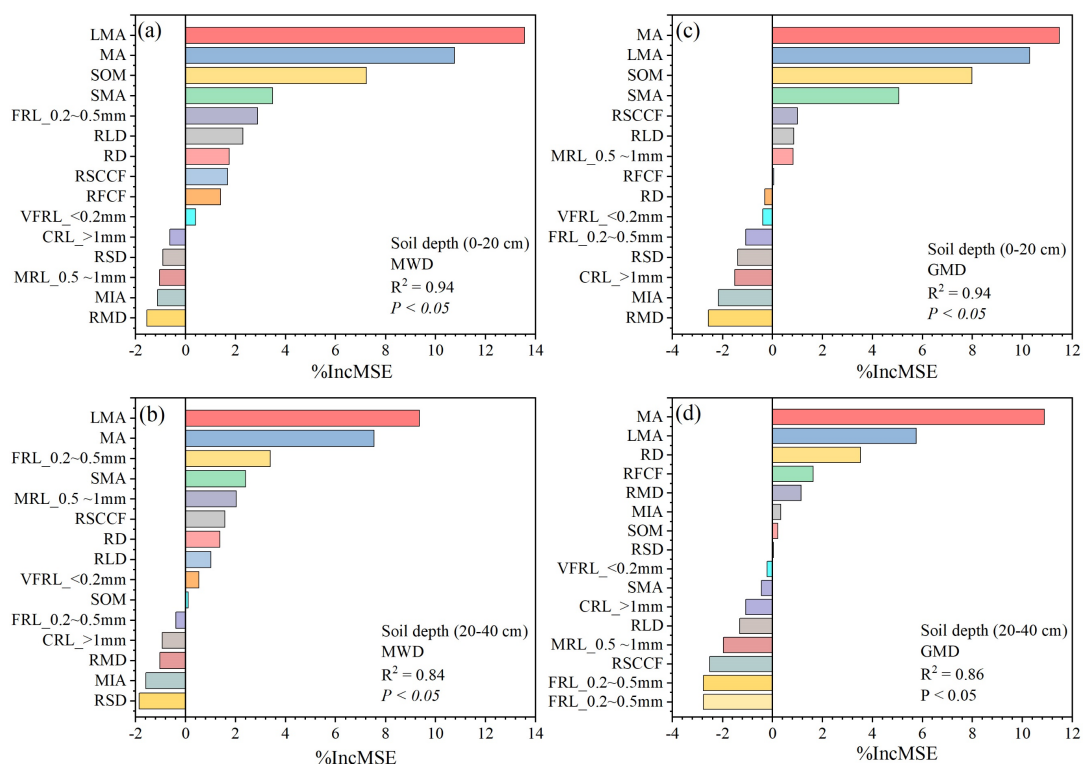
697

698

699

700

701 **Figure. 7.**



702

703

704

705

706

707

708

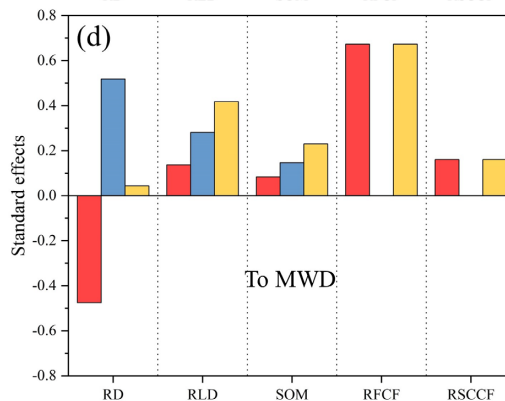
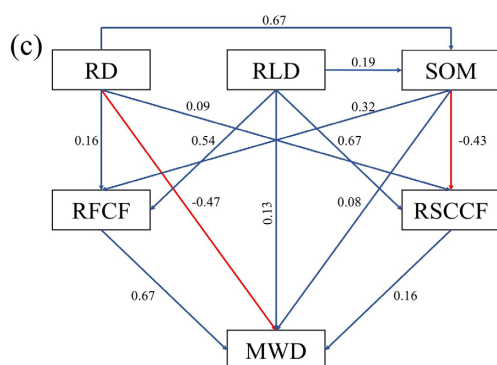
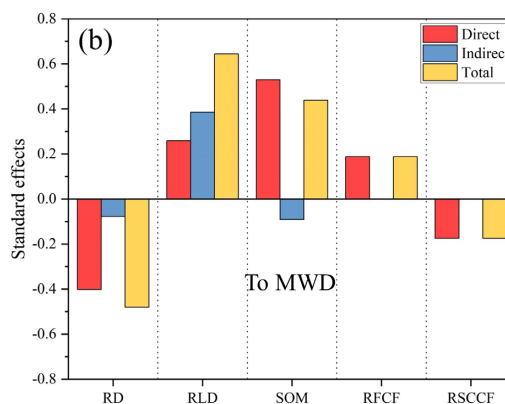
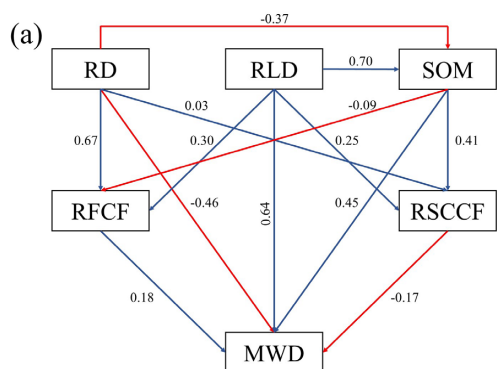
709

710

711

712

713 **Figure 8.**



714